Effects of Cold Plasma on Surface, Thermal and Antimicrobial Release Properties of Chitosan Film

S.K. Pankaj[1], C. Bueno-Ferrer[1], N.N. Misra[1], L. O'Neill[2], Paula Bourke[1] and P.J. Cullen[3]*

[1]*BioPlasma Research Group, School of Food Science and Environmental Health, Dublin Institute of Technology, Cathal Brugha Street, Dublin 1, Ireland*
[2]*FOCAS Research Institute/School of Physics, Dublin Institute of Technology, Kevin Street, Dublin 8, Ireland*
[3]*School of Chemical Engineering, UNSW, Sydney, Australia*

Received November 06, 2015; Accepted March 21, 2016

ABSTRACT: This work aims to analyze the effects of cold atmospheric air plasma treatment of antimicrobial chitosan film with different levels of thymol. Optical characterization of the dielectric barrier discharge showed the generation of reactive nitrogen and oxygen species by the system. A significant increase ($p < 0.05$) in the surface roughness was observed after cold plasma treatment of the films. No significant difference ($p > 0.05$) was observed in the thermal profile of the plasma-treated films. A significant increase ($p < 0.05$) in the thymol diffusion coefficient was observed after the plasma treatment for all the active films.

KEYWORDS: Cold plasma, DBD plasma, antimicrobial packaging, chitosan, thymol, release kinetics

1 INTRODUCTION

Traditionally, roles of packaging materials were limited to containment, protection, convenience and communication without any unwanted interaction with food. However, in recent years, a wide variety of packages and approaches have been employed to interact with the food to provide desirable effects [1]. Active packaging is the approach in which the package, the product, and the environment interact to prolong shelf life or enhance safety or sensory properties, while maintaining the quality of the product [2]. Antimicrobial packaging is a form of active packaging which reduces, inhibits or retards the growth of microorganisms that may be present in the packed food or packaging material itself [3]. Chitosan has gained significant attention in this regard and has been evaluated for numerous applications in the medical, food, agricultural, and chemical industries [4]. Chitosan (poly β-(1→4) N-acetyl-d-glucosamine) is a collective name for the group of partially and fully deacetylated chitin, which is the major constituent of the exoskeleton of crustaceans. Antimicrobial chitosan films prepared by incorporating various organic acids and essential oils have shown the ability to inhibit the growth of various indigenous or inoculated microbes [5, 6]. Essential oils are of great interest as they are naturally obtained from plants, often added to food products as ingredients, and can also serve as active ingredient for antimicrobial packaging systems. Thymol is one of the widely reported essential oils which is abundantly found in thyme (*Thymus vulgaris*) (10–64%) and oregano (*Origanum vulgare*) (traces–64%). It is formed via p-cymene from γ-terpinene and has a very wide spectrum of antibacterial activity [7–10].

Atmospheric cold plasma is a novel nonthermal food technology which has recently drawn considerable interest for decontamination of foods and food processing surfaces [11]. It has shown significant potential for microbial inactivation, retention of food quality and extension of shelf life [12]. Cold plasma is characterized by the disequilibrium of temperature between electrons and ions and can be generated by numerous methods [13]. Dielectric barrier discharge (DBD) is one of the most common methods for generation of nonthermal plasma in which plasma is generated between two parallel metal electrodes where at least one of them is covered by a dielectric layer to limit the discharge current, avoiding an arc transition [14]. DBD plasma has been known to affect the surface and bulk properties of different polymers and its application in food packaging has already been reviewed previously [15].

The aim of this work is to evaluate the effects of cold plasma treatment on surface, thermal and

*Corresponding author: pjcullen@dit.ie

DOI: 10.7569/JRM.2016.634105

antimicrobial release properties of active chitosan film to access its potential to be used in combination with DBD plasma technology for food applications.

2 MATERIAL AND METHODS

2.1 Casting of Active Chitosan Films

Medium molecular weight chitosan (product code: 448877), analytical grade acetic acid and glycerol were purchased from Sigma-Aldrich, Ireland. Chitosan film was prepared by the method followed by Leceta *et al*. [16], with minor modifications. Chitosan (1% w/v) solution was prepared in 1% acetic acid solution. Glycerol (10%) was added after 15 min continuous stirring. Then 2% and 5% of thymol (weight of thymol/weight of dry polymer) (Sigma-Aldrich, Ireland) was added with final stirring for about 30 min until total homogenization of the mixture. As blank, chitosan solutions without active agent were also prepared. Then 70 mL of the film-forming solutions was poured into 15 cm diameter Petri dishes and dried at ambient conditions under laminar flow hood until the solvent was completely evaporated and peeled off after 48 h. The thymol concentration was optimized to 2% and 5% (weight of thymol/weight of dry polymer) to avoid any phase separation during the storage period.

2.2 Dielectric Barrier Discharge Plasma Treatment

The schematic of the experimental setup is presented in Figure 1. Briefly, the DBD plasma source consists of two circular aluminium plate electrodes (outer diameter = 158 mm) over perspex dielectric layers (10 mm thickness). When the potential across the gap reaches the breakdown voltage the dielectric barrier acts as stabilizing material, forming a large number of microdischarges. The applied voltage to the electrode is obtained from a step-up transformer (Phenix Technologies, Inc., USA) using a variac. The input of 230 V, 50 Hz was given to the primary winding of high voltage step-up transformer (Phenix Technologies, Inc., USA) from the main supply. To achieve a stable discharge, a 2 mm thick polypropylene sheet was also used, above which the active chitosan film was placed. The distance between electrodes was 22 mm. The atmospheric air condition at the time of treatment was 50% relative humidity (RH) and 22 °C, as measured using a humidity-temperature probe connected to a data logger (Testo 176 T2, Testo Ltd., UK). Samples were treated at 70 kV for 5 minutes.

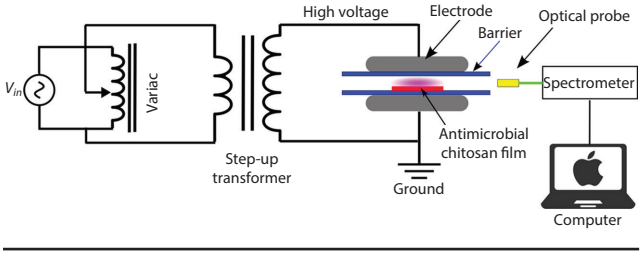

Figure 1 Schematic of the experimental setup for DBD plasma treatment (not to scale).

2.3 Optical Emission Spectroscopy

For plasma diagnostics and information about the reactive species generated by the discharge, optical emission spectra were recorded using a spectrometer (Ocean Optics HR 2000+) at 0.5 nm resolution over the wavelength range of 200 to 800 nm. The emission from the discharge was coupled to the spectrometer using an optical fiber (0.22 numerical aperture, 600 µm core, 30 cm length, from OZ Optics). The integration time was 5000 ms and 5 samples were collected; spectra were noise cancelled and averaged to obtain the representative spectrum. The spectrum was analyzed using the National Institute of Standards and Technology (NIST) atomic spectra database [17] and published works [18] for identification of active chemical species in the discharge.

2.3 Thymol Release

Thymol release was measured by the method described by Del Nobile *et al*. [19], with slight modifications. The prepared active films were put into a glass beaker with 250 mL of distilled water (volume/surface ratio 4.5 mL cm^{-2}) and shaken at 25 °C and 150 rpm in an orbital shaker for 50 hours. The thymol release kinetics was evaluated by monitoring thymol concentration in the surrounding solution using HPLC (Waters e2695 Separation Module and Waters 2998 Photodiode Array Detector, Waters Corporation, Ireland), until equilibrium value was achieved. The chromatographic column used was a C18 reverse phase column, 250 × 4 mm, particle size 5 µm. A linear gradient elution with acetonitrile-0.05 M orthophosphoric acid was used [20]. Typical gradient used is given in Table 1. The flow rate was 1 mL min^{-1} with injection volume of 5 µl and the elution was detected at a wavelength of 277 nm. The calibration curve was constructed for peak area against thymol concentration of standard solutions from 10 to 500 ppm.

2.4 Atomic Force Microscopy (AFM)

Atomic force microscopy measurements were carried out to observe the surface characteristics of the control

Table 1 Gradient elution for determination of thymol.

Time (min)	Acetonitrile	0.05M orthophosphoric acid
0	40	60
7	46	54
8	60	40
11	60	40
20	40	60

and plasma-treated samples. The AFM used was MFP-3D BIO 1126 (Asylum Research, Santa Barbara, CA, USA) operated in intermittent contact (tapping) mode. The images were collected at a fixed scan rate of 0.5 Hz. The sampling rate was 512 lines. Data were processed using MF3D software (version 111111+1219).

2.5 Thermogravimetric Analysis (TGA)

The TGA analyses were performed with a Mettler Toledo thermal analyzer, model TGA/SDTA 851e (Schwarzenbach, Switzerland). Approximately 3 g samples were heated at 10 °C min^{-1} from 30 to 700 °C under nitrogen atmosphere (flow rate 50 mL min^{-1}). Initial degradation temperature (T_5) was determined as the temperature at which 5% mass loss was observed.

2.6 Statistical Analysis

Analysis of variance was done for all analyses and treatments and significance of difference was assessed using Tukey's comparison tests at significance levels of $p \leq 0.05$. Analysis was carried out in SPSS statistical package (SPSS Inc., Chicago, USA). The mathematical model for thymol release kinetics was performed in Matlab 2012a (MathWorks, USA).

3 RESULTS AND DISCUSSION

3.1 Emission Characteristics of the Discharge

The emission spectrum of the electrical discharge in air is presented in Figure 2. The optical spectrograph reveals predominant peaks in the near ultraviolet region of the spectrum which correspond to emissions from excited or ionic molecular nitrogen species, which form by the excitation and dissociation of the nitrogen molecules in the gas phase. Most of the emissions were attributed to N_2 2+ system (second positive system, SPS): $C^3\Pi_u - B^3\Pi_g$: (1–0) at 317.5 nm, (0–0) at 336.8 nm, (0–1) 356.3 nm, and (0–2) 379.9 nm [21] and N_2^+1- system (first negative system,

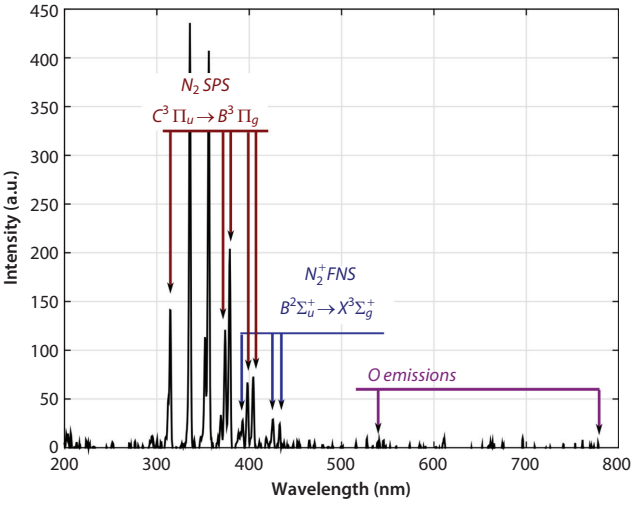

Figure 2 Optical emission spectrum of the discharge in air.

FNS): $N_2^+B^2\Sigma_u^+ \rightarrow X_2\Sigma_g^+$, with the main band head at 391.6 nm. The OH excitation rendered itself as a minor peak at about 300 nm despite the presence of water vapors (RH = 22%) due to the loss of the OH ($A^2\Sigma^+$) state resulting from radiative de-excitation and collisional quenching [18]. Similarly, peaks associated with optical transitions of the O atom were also observed at very low intensities at 725.4 nm and 777.4 nm. The plasma source employed in this work also generates considerable amounts of ozone, further details on which can be found from our earlier studies [22, 23]. The ozone formation is a three body collision reaction given by [24]:

$$O + O_2 + M \rightarrow O_3^* + M \rightarrow O_3$$

where M is the third collision partner (O_2, O_3, O or N_2). Altogether, the DBD plasma discharge chemistry resulted in generation of several excited nitrogen and reactive oxygen species in the gas phase.

3.2 Surface Characteristics

The surface topographies of control and plasma-treated active chitosan films by atomic force microscopy (AFM) are shown in Figure 3. The roughness parameters for the control and plasma-treated film surfaces are presented in Table 2. It is clear from these results that the DBD plasma treatment leads to an increase in the surface roughness of chitosan films. The surface topography of untreated active chitosan films was observed to be smooth and homogenous with root mean square roughness (Rrms) of 7.2 nm. The Rrms of DBD plasma-treated films at 70 kV for 5 min was found to be significantly ($p < 0.05$) higher

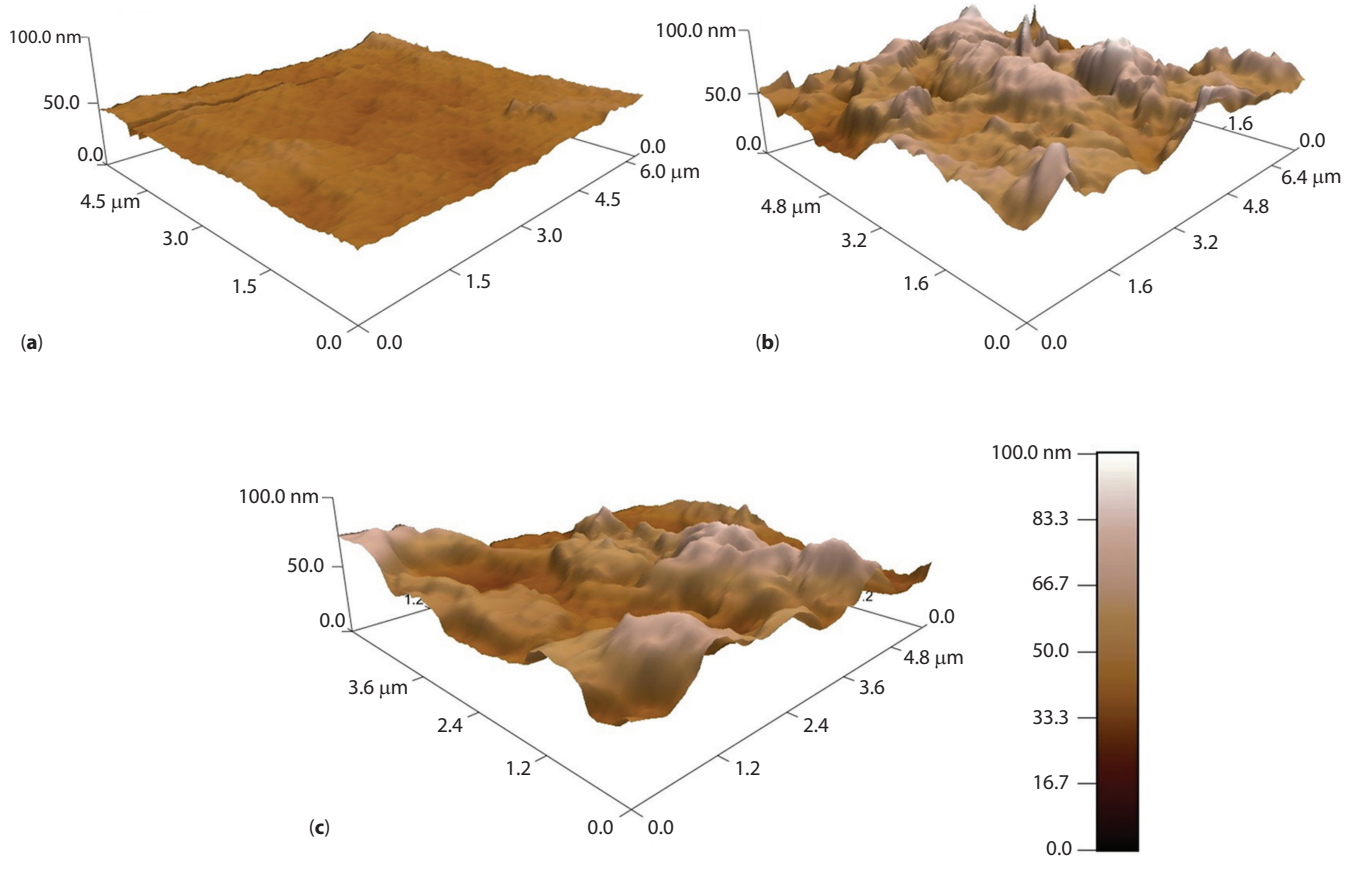

Figure 3 AFM images of the surface of (**a**) untreated, (**b**) plasma-treated active chitosan (2%) and (**c**) plasma-treated active chitosan (5%) films.

Table 2 Roughness parameters for untreated and plasma-treated active chitosan films (R_{RMS}: root mean square roughness, R_{Peak}: highest peak, R_{Groove}: lowest groove).

Characteristics	Untreated active chitosan film	Plasma-treated active chitosan film (2%)	Plasma-treated active chitosan film (5%)
R_{RMS} (nm)	7.19	13.98	10.87
R_{Peak} (nm)	7.40	46.84	33.71
R_{GROOVE} (nm)	–20.13	–24.51	–20.33
Skew	0.342	0.115	0.784
Kurtosis	0.787	0.059	0.109

than the untreated film. The increase in surface roughness after DBD plasma treatment can be attributed to the etching effect of DBD plasma, which is consistant with results reported previously [15]. Etching by DBD plasma can be due to chemical etching by breaking of bonds, chain scission, chemical degradation or physical processes by physical removal of low molecular weight fragments. While chemical etching is promoted by radicals in plasma discharges, physical etching occurs under strong bombardment by energetic particles such as electrons and ions [25, 26]. Although etching effects after plasma treatment have many applications in the packaging industry, they also have the potential to be used for controlling the release kinetics of active compounds from an active packaging film [27].

3.3 Thermal Properties

Thermogravimetric analysis was carried out in order to analyze the weight loss as a function of temperature for control and plasma-treated active chitosan

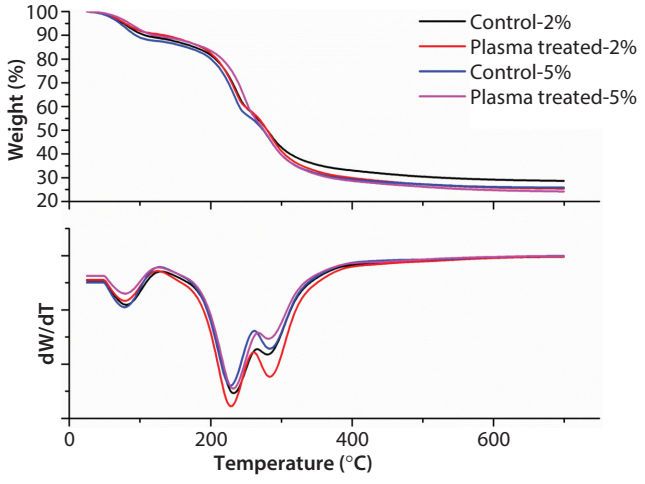

Figure 4 Thermogravimetric results for control and plasma-treated active chitosan films.

films and the results are shown in Figure 4. Three different thermal behavior regions were observed in the TGA profile of all the active chitosan films. The slight weight loss below 100 °C was attributed to the moisture content of the samples. The weight loss was observed at 220 °C, which can be associated with glycerol evaporation [28]. No significant difference ($p > 0.05$) was observed for the main stage weight loss due to the thermal and oxidative decomposition, vaporization and elimination of volatile products of chitosan at 285 °C [29].

3.4 Release Kinetics of Thymol

There are many approaches to determine the diffusion of additives from an active packaging film in food simulants which have been widely reported previously [30–32]. In the present study, it was assumed that the process occurred in a thin sheet of the active film, initially having a homogeneous thymol concentration distribution. Solvent absorption and solute diffusion occurred simultaneously and the thickness of the active film was considered to be very small in comparison with the width, so diffusivity was considered unidirectional and perpendicular to the surface of the sheet. When the film comes in contact with aqueous solution, first the water molecules penetrate into the matrix, leading to its swelling and making the meshes of the polymeric network wider, allowing the active compound to diffuse through the matrix into the outer solution until a thermodynamic equilibrium between the outer solution and polymer is reached [27]. Fick's second law of diffusion describes species concentration change as a function of time and position. For

Table 3 Parameters obtained by fitting Equation 2 to experimental data. Values represented as Mean ± Standard deviation. Means, which are not followed by a common superscript letter, are significantly different ($p \leq 0.05$).

Active chitosan films	D ($cm^2.s^{-1}$)	M_{eq} (ppm)
2%-Control	4.47×10^{-7a}	5.91 ± 0.41^a
2%-Plasma treated	7.70×10^{-7b}	5.80 ± 0.20^a
5%-Control	3.14×10^{-7c}	13.70 ± 1.34^b
5%-Plasma treated	6.18×10^{-7d}	13.78 ± 0.85^b

unidirectional diffusion, one-dimensional linear partial differential equation can be written as [33]:

$$\frac{\delta C}{\delta t} = D(t)\frac{\partial^2 C}{\partial x^2} \quad (1)$$

where C is the concentration of solute; D is diffusivity; x is the coordinate dimension in the direction of transport; and t is time.

Since the aim of this work was to assess the change in the thymol release kinetics due to DBD plasma treatment, a simple approach, such as reported by Yoshida *et al.* [32], has been used. Based on that, Fick's second law intended for a plane sheet with constant boundary condition and uniform initial concentration can be solved by Fourier series method and integrated over time and space to give Equation 2.

$$M(t) = M_{eq}\left[1 - \frac{8}{\pi^2}\sum_{n=0}^{\infty}\frac{1}{(2n+1)^2}.\exp\left\{\frac{-D.(2n+1)^2.\pi^2.t}{h^2}\right\}\right] \quad (2)$$

where $M(t)$ is the amount of thymol released (ppm) at time t (h); M_{eq} is the amount of thymol released at equilibrium conditions (ppm); D is the thymol diffusion coefficient (cm^2s^{-1}) through the swollen polymeric matrix; and h is the film thickness (cm).

The parameters after fitting the experimental values to Equation 2 are reported in Table 3. As clearly seen, a significant increase ($p < 0.05$) in the thymol diffusion coefficient after DBD plasma treatment was observed for both active films with different thymol concentration levels. The equilibrium thymol concentration in the solution was reached within 60 h and was different after DBD plasma treatment. The equilibrium thymol concentrations for 2% and 5% thymol-containing chitosan film were 5.9 ppm and 13.7 ppm respectively (Figure 5). The increase in the diffusion rate of thymol after DBD plasma treatment can be correlated with the etching effect leading to the increase in surface roughness, which in turn reduced the effective

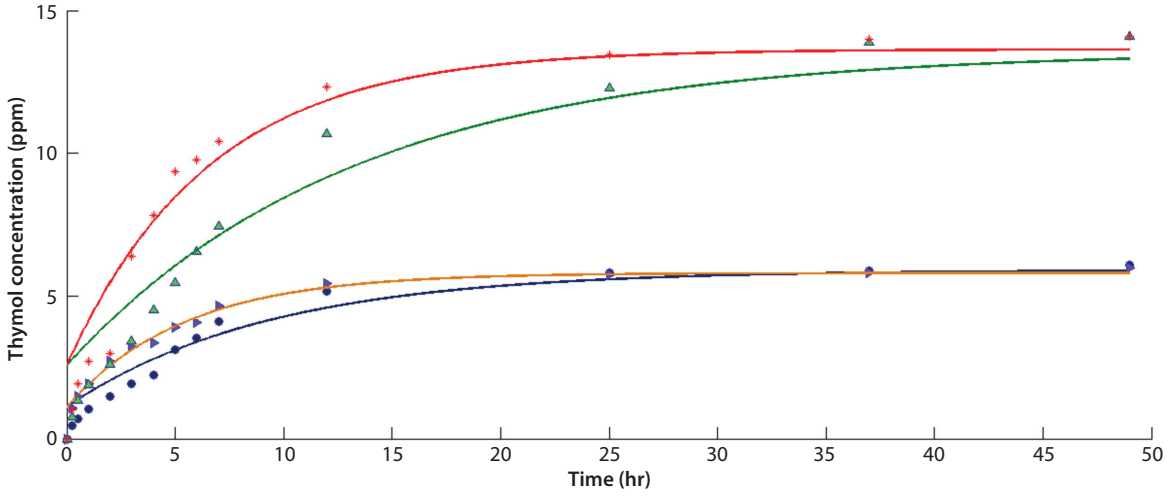

Figure 5 Release kinetics of thymol from chitosan films after plasma treatment in water. (●) 2% Control, (►) 2% Plasma treated, (▲) 5% Control, (+) 5% Plasma treated. The curves are the fitting experimental data to Equation 2.

film thickness and exposed thymol for an accelerated release from the active film [27].

4 CONCLUSION

This study showed the effect of DBD plasma treatment on antimicrobial chitosan films containing thymol as an active ingredient. The optical spectra of the dielectric barrier discharge showed the generation of reactive nitrogen and oxygen species by the plasma system. Cold plasma treatment significantly increased ($p < 0.05$) the surface roughness of films due to the etching effects. No significant difference ($p > 0.05$) was observed in the thermal properties of the plasma-treated films. Also, no evidence of thermal decomposition, vaporization or elimination of volatiles was observed after the plasma treatment. A significant increase ($p < 0.05$) in the thymol diffusion coefficient was observed after the plasma treatment for all the active films. The ability to control the antimicrobial release from the packaging film could serve as an important tool for the food industry to extend the shelf life of food products in an environment-friendly manner.

REFERENCES

1. D.S. Cha and M.S. Chinnan, Biopolymer-based antimicrobial packaging: A review. *Crit. Rev. Food Sci. Nutr.* **44**(4), 223–237 (2004).
2. P. Suppakul, J. Miltz, K. Sonneveld, and S.W. Bigger, Active packaging technologies with an emphasis on antimicrobial packaging and its applications. *J. Food Sci.* **68**(2), 408–420 (2003).
3. P. Appendini and J.H. Hotchkiss, Review of antimicrobial food packaging. *Innov. Food Sci. & Emerg. Technol.* **3**(2), 113–126 (2002).
4. S. Zivanovic, S. Chi, and A.F. Draughon, Antimicrobial activity of chitosan films enriched with essential oils. *J. Food Sci.* **70**(1), M45–M51 (2005).
5. M. Aider, Chitosan application for active bio-based films production and potential in the food industry: Review. *LWT-Food Sci. Technol.* **43**(6), 837–842 (2010).
6. P.K. Dutta, S. Tripathi, G.K. Mehrotra, and J. Dutta, Perspectives for chitosan based antimicrobial films in food applications. *Food Chem.* **114**(4), 1173–1182 (2009).
7. S. Burt, Essential oils: Their antibacterial properties and potential applications in foods—a review. *Int. J. Food Microbiol.* **94**(3), 223–253 (2004).
8. M. Marino, C. Bersani, and G. Comi, Antimicrobial activity of the essential oils of *Thymus vulgaris* L. measured using a bioimpedometric method. *J. Food Protect.* **62**(9), 1017–1023 (1999).
9. S. Kokkini, R. Karousou, A. Dardioti, N. Krigas, and T. Lanaras, Autumn essential oils of Greek oregano. *Phytochemistry* **44**(5), 883–886 (1997).
10. H.J.D. Dorman and S.G. Deans, Antimicrobial agents from plants: Antibacterial activity of plant volatile oils. *J. Appl. Microbiol.* **88**(2), 308–316 (2000).
11. S.K. Pankaj, N.N. Misra, and P.J. Cullen, Kinetics of tomato peroxidase inactivation by atmospheric pressure cold plasma based on dielectric barrier discharge. *Innov. Food Sci. & Emerg. Technol.* **19**, 153–157 (2013).
12. S.K. Pankaj, C. Bueno-Ferrer, N. Misra, L. O'Neill, B. Tiwari, P. Bourke, and P. Cullen, Dielectric barrier discharge atmospheric air plasma treatment of high amylose corn starch films. *LWT-Food Sci. Technol.* **63**(2), 1076–1082 (2015).
13. S.K. Pankaj, C. Bueno-Ferrer, N.N. Misra, P. Bourke, and P.J. Cullen, Zein film: Effects of dielectric barrier discharge atmospheric cold plasma. *J. Appl. Polym. Sci.* **131**(18), 1–6 (2014).

14. S.K. Pankaj, C. Bueno-Ferrer, N.N. Misra, L. O'Neill, B.K. Tiwari, P. Bourke, and P.J. Cullen, Physicochemical characterization of plasma-treated sodium caseinate film. *Food Res. Int.* **66**, 438–444 (2014).
15. S.K. Pankaj, C. Bueno-Ferrer, N.N. Misra, V. Milosavljević, C.P. O'Donnell, P. Bourke, K.M. Keener, and P.J. Cullen, Applications of cold plasma technology in food packaging. *Trends Food Sci. Tech.* **35**(1), 5–17 (2014).
16. I. Leceta, P. Guerrero, I. Ibarburu, M.T. Dueñas, and K. de la Caba, Characterization and antimicrobial analysis of chitosan-based films. *J. Food Eng.* **116**(4), 889–899 (2013).
17. National Institute of Standards and Technology, Atomic spectra database, cited June 9, 2013, Available from: http://physics.nist.gov/PhysRefData/ASD/index.html (2012).
18. N.N. Misra, K.M. Keener, P. Bourke, J.P. Mosnier, and P.J. Cullen, In-package atmospheric pressure cold plasma treatment of cherry tomatoes. *J. Biosci. Bioeng.* **118**(2), 177–182 (2014).
19. M.A. Del Nobile, A. Conte, A.L. Incoronato, and O. Panza, Antimicrobial efficacy and release kinetics of thymol from zein films. *J. Food Eng.* **89**(1), 57–63 (2008).
20. A.-C. Martel and S. Zeggane, Determination of acaricides in honey by high-performance liquid chromatography with photodiode array detection. *J. Chromatogr. A* **954**(1–2), 173–180 (2002).
21. P.J. Cullen and V. Milosavljevi, Spectroscopic characterization of a radio-frequency argon plasma jet discharge in ambient air. *Progr. Theor. Exp. Phys.* **2015**(6), 63J01 (2015).
22. N.N. Misra, T. Moiseev, S. Patil, S.K. Pankaj, P. Bourke, J.P. Mosnier, K.M. Keener, and P.J. Cullen, Cold plasma in modified atmospheres for post-harvest treatment of strawberries. *Food Bioprocess Tech.* **7**(10), 3045–3054 (2014).
23. T. Moiseev, N.N. Misra, S. Patil, P.J. Cullen, P. Bourke, K.M. Keener, and J.P. Mosnier, Post-discharge gas composition of a large-gap DBD in humid air by UV–Vis absorption spectroscopy. *Plasma Sources Sci. Technol.* **23**(6), 65033–65045 (2014).
24. B. Eliasson, M. Hirth, and U. Kogelschatz, Ozone synthesis from oxygen in dielectric barrier discharges. *J. Phys. D: Appl. Phys.* **20**, 1421–1437 (1987).
25. Y. Akishev, M. Grushin, N. Dyatko, I. Kochetov, A. Napartovich, N. Trushkin, T. Minh Duc, and S. Descours, Studies on cold plasma–polymer surface interaction by example of PP- and PET-films. *J. Phys. D: Appl. Phys.* **41**(23), 235203, 1–13 (2008).
26. S. Mirabedini, H. Arabi, A. Salem, and S. Asiaban, Effect of low-pressure O_2 and Ar plasma treatments on the wettability and morphology of biaxial-oriented polypropylene (BOPP) film. *Prog. Org. Coat.* **60**(2), 105–111 (2007).
27. S.K. Pankaj, C. Bueno-Ferrer, N.N. Misra, L. O'Neill, A. Jiménez, P. Bourke, and P.J. Cullen, Surface, Thermal and antimicrobial release properties of plasma-treated zein films. *J. Renew. Mater.* **2**(1), 77–84 (2014).
28. I. Leceta, M. Peñalba, P. Arana, P. Guerrero, and K. de la Caba, Ageing of chitosan films: Effect of storage time on structure and optical, barrier and mechanical properties. *Eur. Polym. J.* **66**, 170–179 (2015).
29. C.G.T. Neto, J.A. Giacometti, A.E. Job, F.C. Ferreira, J.L.C. Fonseca, and M.R. Pereira, Thermal analysis of chitosan based networks. *Carbohydr. Polym.* **62**(2), 97–103 (2005).
30. J.H. Han and J.D. Floros, Simulating diffusion model and determining diffusivity of potassium sorbate through plastics to develop antimicrobial packaging films. *J. Food Process. Preserv.* **22**(2), 107–122 (1998).
31. H. Ortiz-Vazquez, J. Shin, H. Soto-Valdez, and R. Auras, Release of butylated hydroxytoluene (BHT) from Poly(lactic acid) films. *Polym. Test.* **30**(5), 463–471 (2011).
32. C.M.P. Yoshida, C.E.N. Bastos, and T.T. Franco, Modeling of potassium sorbate diffusion through chitosan films. *LWT-Food Sci. Technol.* **43**(4), 584–589 (2010).
33. J. Crank, *The Mathematics of Diffusion*, 2nd ed., Oxford University Press, New York, NY (1975).